

Supplementary Figures

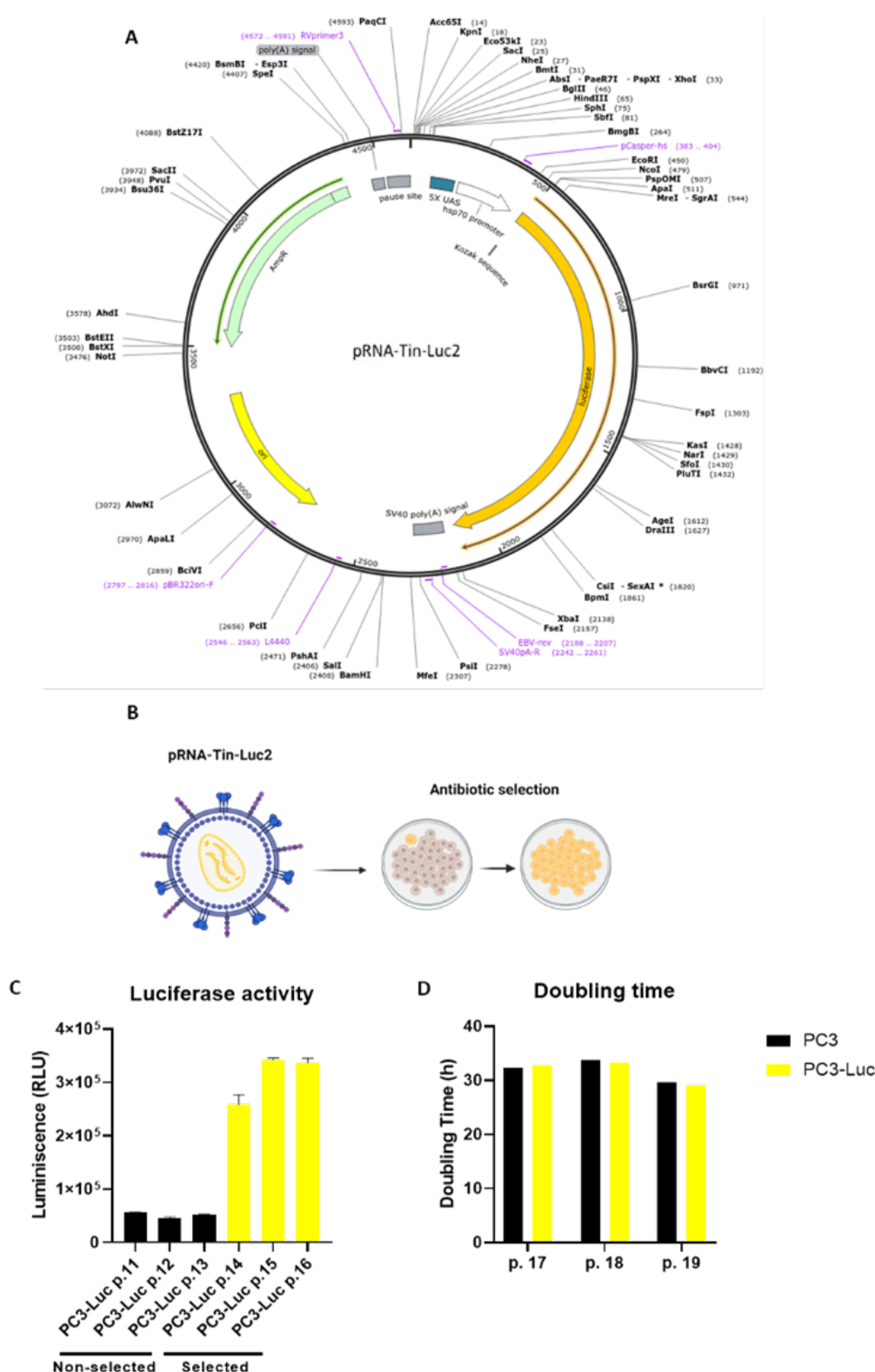


Figure S1. Lentiviral Infection of PC3 Prostate Cancer Cells with the Luciferin Transgene. **A)** The pRNATin-Luc2 plasmid expresses the Luciferase transgene under the control of the T3 promoter and a G418 (geneticin) antibiotic resistance cassette. **B)** PC3 cells were infected with lentiviral particles containing the pRNATin-Luc2 plasmid, and luciferase-positive cells (PC3-Luc cells) were selected using G418. **C)** Luminescence analysis of luciferase expression demonstrates efficient and stable transfection. **D)** Doubling time of PC3 and PC3-Luc cell lines for three different

passages. Data expressed as mean \pm SEM (n = 3). Abbreviations- RLU: relative luminescence units.

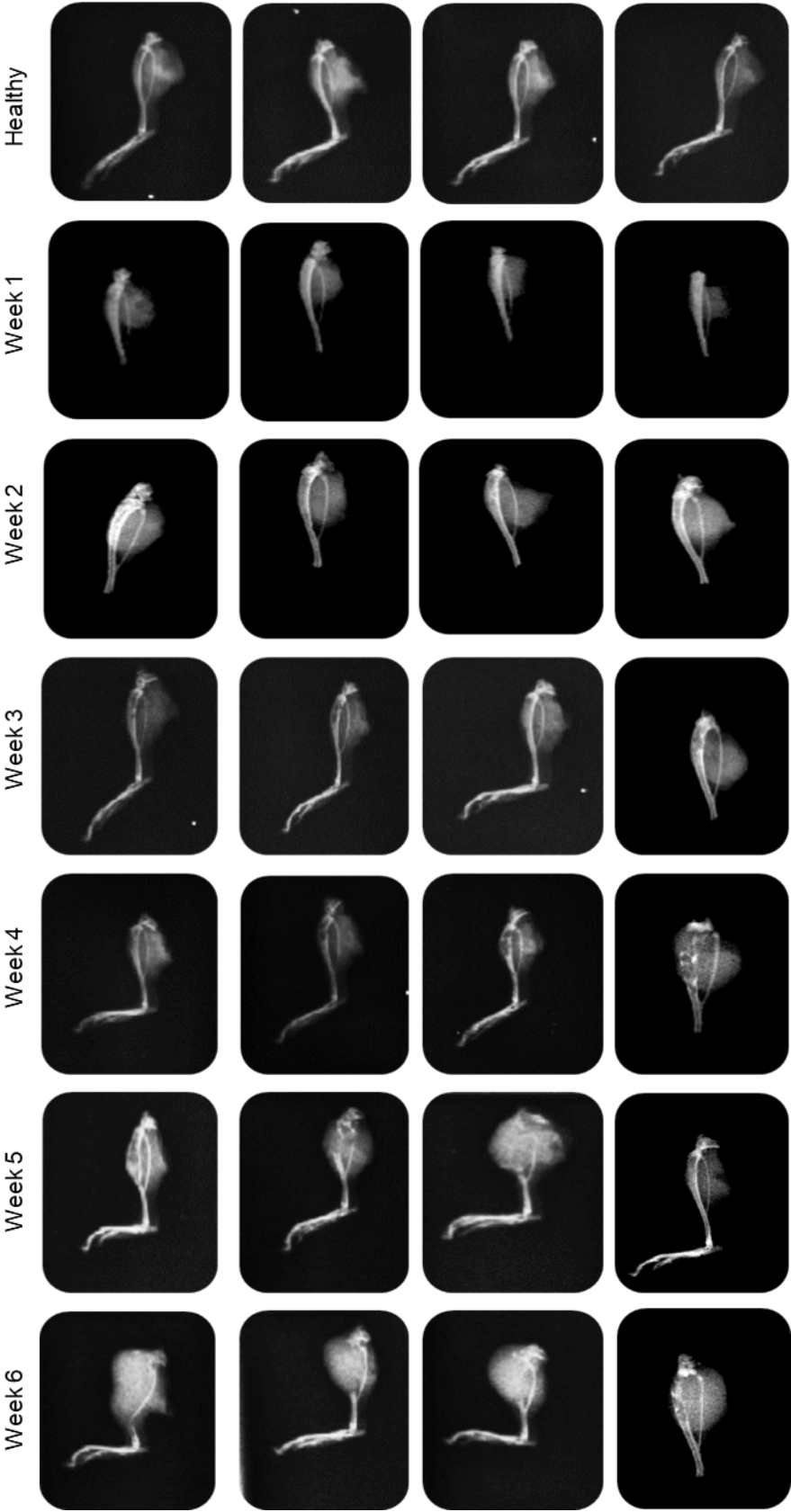


Figure S2. X-ray image data for the 6 weeks of tumor development. Representative images of IVIS Spectrum X-ray data covering 6 weeks of tumor development following the injection of PC3-Luc cells into the left tibia.

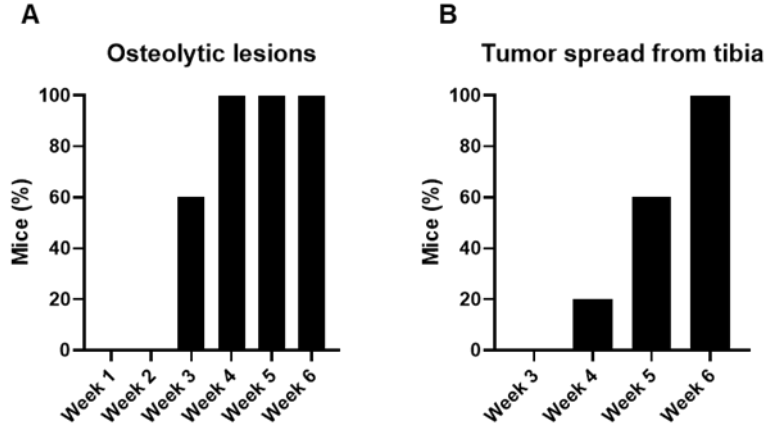


Figure S3. Quantification of osteolytic lesion from X-ray data. A) Percentage of mice with osteolytic lesions in X-ray images from weeks 1 to 6 and B) percentage of mice presenting osteolytic lesions that break the tibia (n = 4).

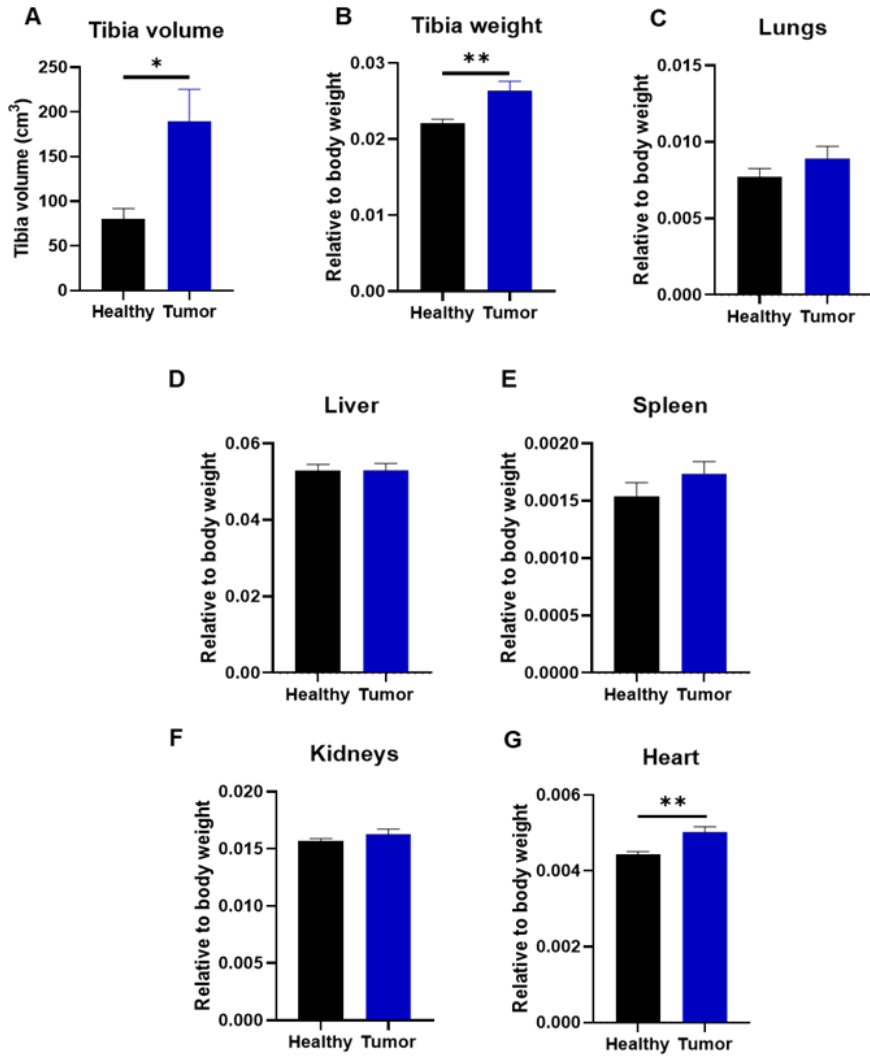


Figure S4. Organ measurements at the experimental endpoint. **A)** Volume of healthy and tumor-affected tibias (in cm^3) at the experimental endpoint ($n = 4$). **B-G)** The weight of **B)** healthy and tumor-affected tibias and the **C)** lung, **D)** liver, **E)** spleen, **F)** kidney, and **G)** heart relative to the total body weight of healthy control mice and tumor mice at the experimental endpoint ($n \geq 8$). Data expressed as mean \pm SEM. Statistical analysis performed using ANOVA, * $p < 0.05$, ** $p < 0.01$.

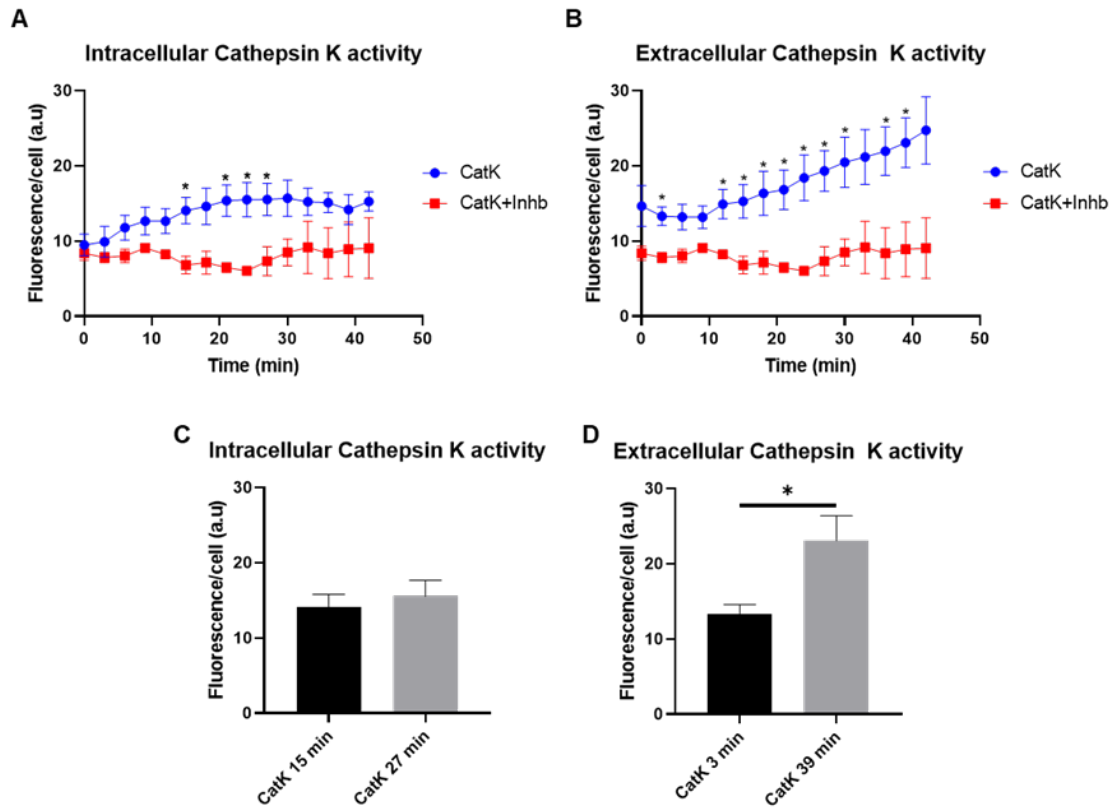


Figure S5. Cathepsin K Activity Determination in PC3-Luc cells. **A and B)** Measurement of **A)** intracellular and **B)** extracellular cathepsin K activity over time measured using a cathepsin K substrate in the presence/absence of a cathepsin K inhibitor (Leupeptin). **C)** Comparison of intracellular cathepsin K activity at the first significant point (15 min) and last significant point (27 min) ($n = 3$). **D)** Comparison of extracellular cathepsin K activity at the first significant point (3 min) and last significant point (39 min) ($n = 3$). Abbreviations - A.U.: arbitrary units. Data expressed as mean \pm SEM. Statistical analysis performed using ANOVA, * $p < 0.05$.

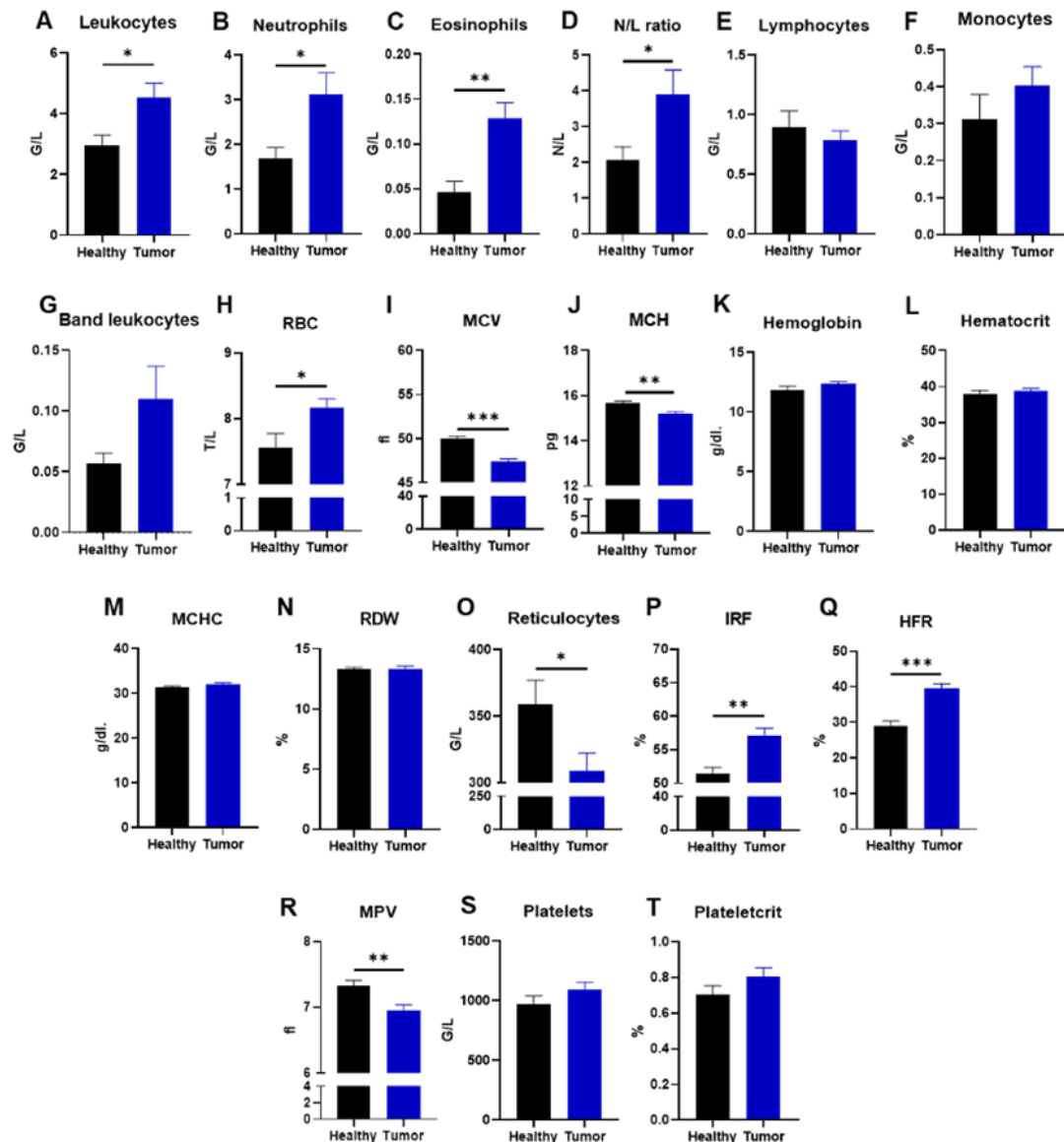


Figure S6. Hematological Analysis of the Bone Metastatic Prostate Cancer Mouse Model at the Experimental Endpoint. Analysis of **A)** leukocytes, **B)** neutrophils, **C)** eosinophils, **D)** the neutrophil-to-lymphocyte ratio (N/L), **E)** lymphocytes, **F)** monocytes, **G)** band leukocytes, **H)** red blood cells (RBC), **I)** mean corpuscular volume (MCV), **J)** mean corpuscular hemoglobin (MCH), **K)** hemoglobin, **L)** hematocrit, **M)** mean corpuscular hemoglobin concentration (MCHC), **N)** red cell distribution width (RDW), **O)** reticulocytes, **P)** immature reticulocyte fraction (IRF), **Q)** the reticulocyte high-fluorescence ratio (HFR), **R)** mean platelet volume (MCV), **S)** platelets and **T)** plateletcrit at the experimental endpoint (week 4). Abbreviations - B: bone; BM: bone marrow; fL: femtoliter; G/L: grams per liter; N/L: neutrophil-to-lymphocyte ratio; pg: pictograms; star: tumor; T/L: tera per liter. Data expressed as mean±SEM (n ≥ 8). Statistical analysis performed using ANOVA, *p < 0.05, **p < 0.01, ***p < 0.001.

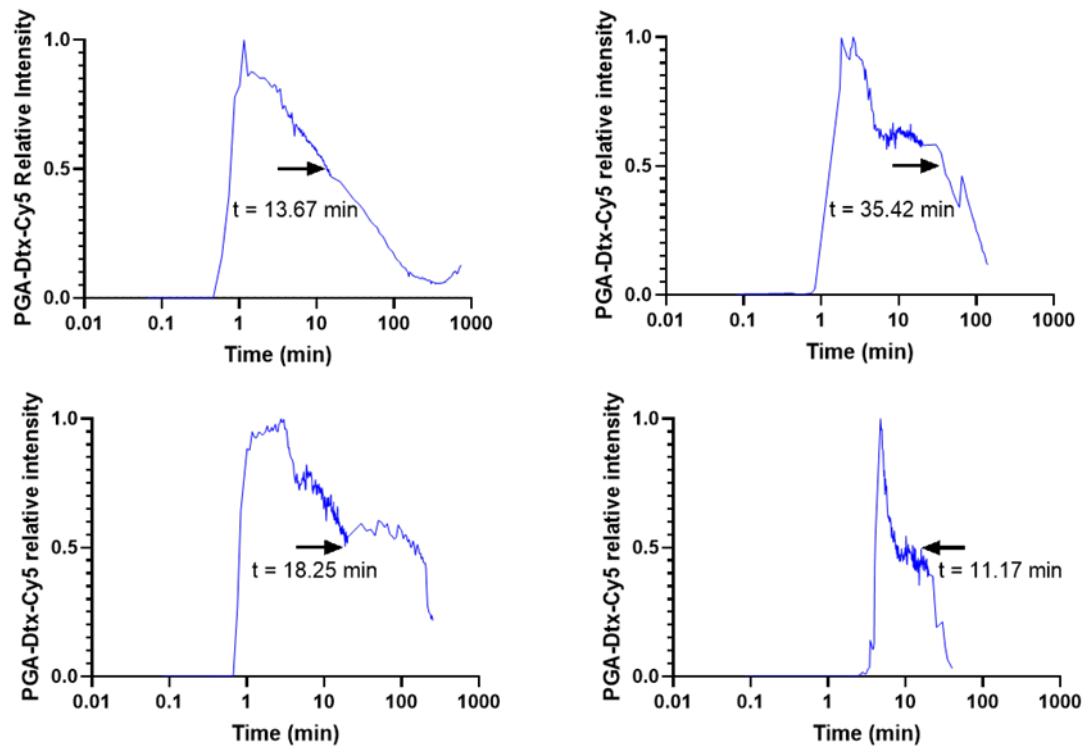


Figure S7. Circulation Analysis Following Cy5.5-labeled PGA-Dtx Administration. Fluorescence intensity of the Cy5.5-labeled PGA-Dtx over time in the ear artery in four different mice.

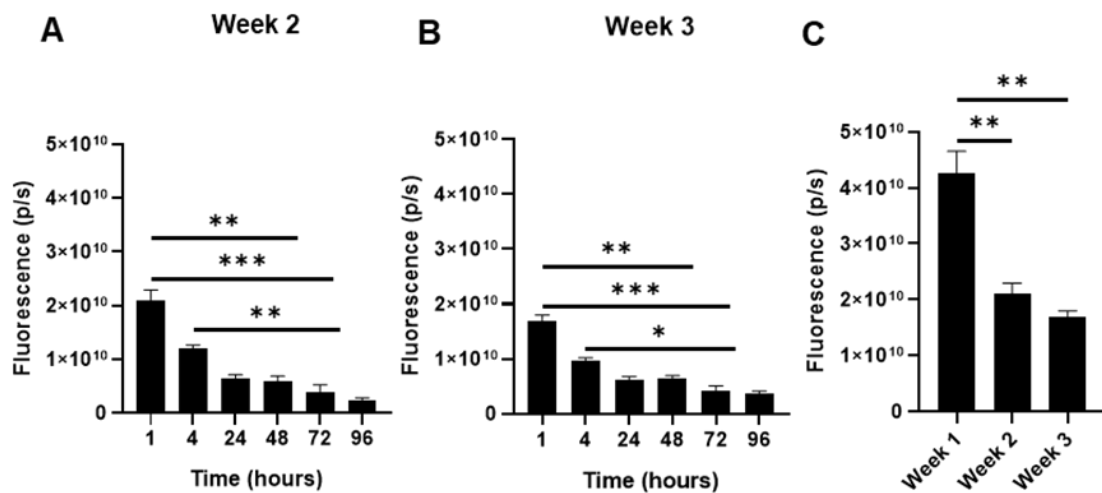


Figure S8. PGA-Dtx Pharmacokinetics. **A and B)** Relative fluorescence intensity of Cy5.5-labeled PGA-Dtx over time after intravenous injection at **A)** weeks 2 and **B)** 3. **C)** Relative fluorescence intensity of Cy5.5-labeled PGA-Dtx 1 h after intravenous injection at weeks 1, 2, and 3. Data expressed as mean ± SEM (n = 6). Statistical analysis performed using ANOVA, *p < 0.05, **p < 0.01, ***p < 0.001.

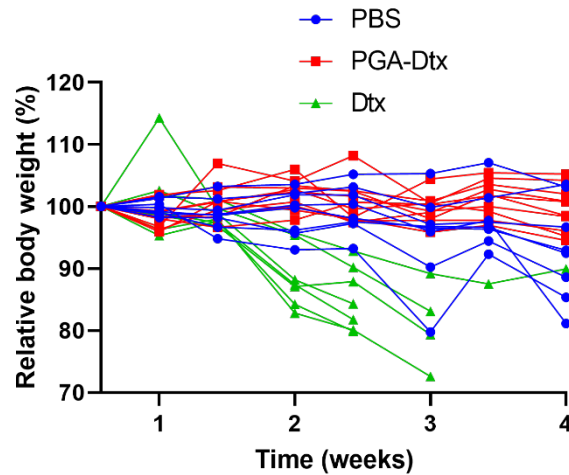


Figure S9. Relative body weight percentage alterations for PBS-, PGA-Dtx and free Dtx-treated individual mice over time (n ≥ 8).

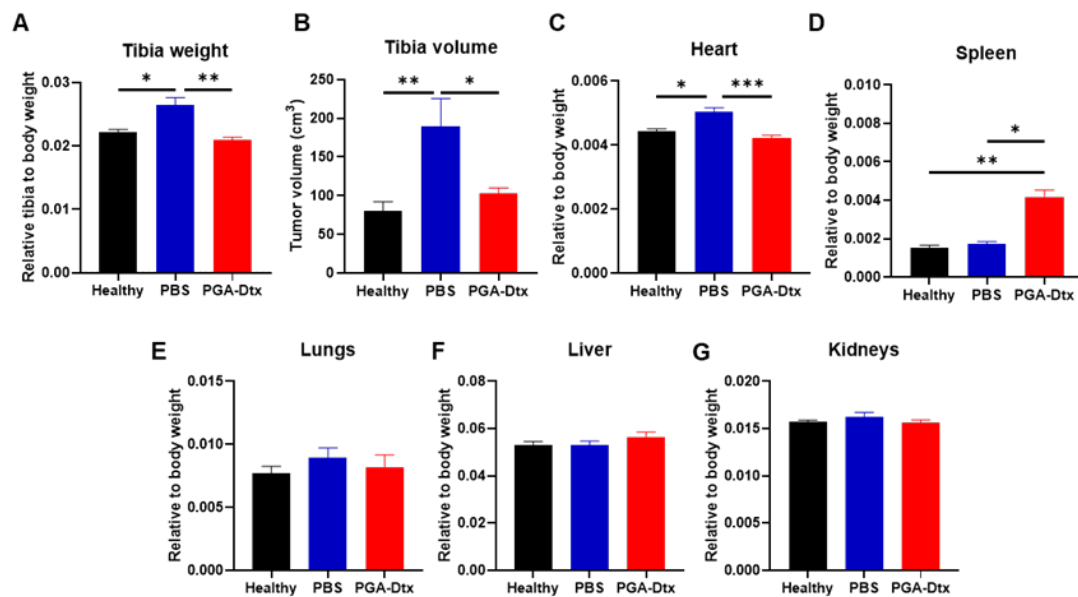


Figure S10. Organ measurements after PGA-Dtx treatment at the experimental endpoint. A) Tumor weight expressed relative to total body weight at week 4 in healthy, PBS-treated, and PGA-Dtx-treated mice. B) Tumor volume expressed in cm³ at week 4 in healthy, PBS-treated, and PGA-Dtx-treated mice. C) Heart, D) spleen, E) lungs, F) liver, and G) kidney weight expressed relative to total body weight at week 4 in healthy, PBS-treated, and PGA-Dtx-treated mice. Data expressed as mean ± SEM (n ≥ 6). Statistical analysis performed using ANOVA, *p < 0.05, **p < 0.01, ***p < 0.001.

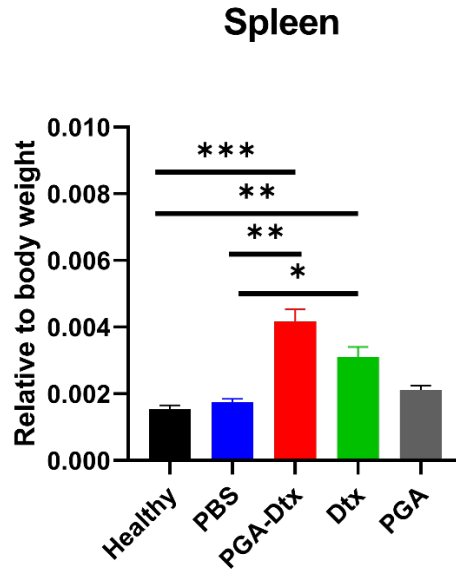


Figure S11. Spleen measurements after treatment. Spleen weight expressed relative to total body weight in healthy, PBS-treated, PGA-Dtx- and PGA-treated mice at experimental endpoint and in free Dtx-treated mice at the time of mouse death. Data expressed as mean \pm SEM ($n \geq 6$). Statistical analysis performed using ANOVA, * $p < 0.05$, ** $p < 0.01$, *** $p < 0.001$.

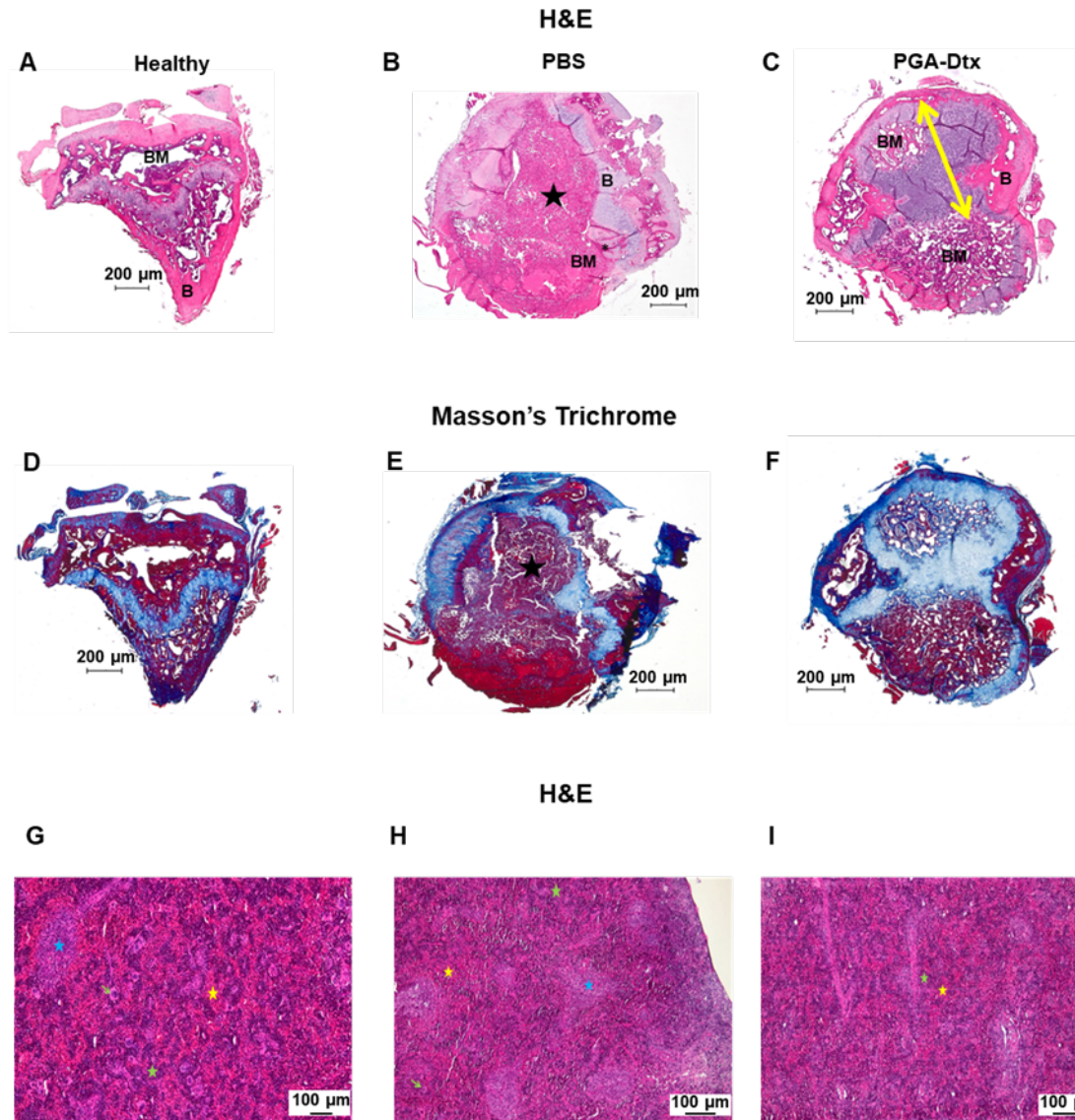


Figure S12. Histological Analysis in the Bone Metastatic Prostate Cancer Mouse Model Following PGA-Dtx Treatment. **A-C)** Hematoxylin and eosin (H&E) staining of **A)** healthy and tumor-affected tibias of **B)** PBS-treated and **C)** PGA-Dtx-treated mice at the experimental endpoint. **D-F)** Masson's trichrome staining of **D)** healthy and tumor-affected tibias of **E)** PBS-treated and **F)** PGA-Dtx-treated mice at the experimental endpoint (black star: tumor; yellow arrow: chondral metaplasia). **G-I)** H&E staining of the spleen of **G)** healthy mice and **H)** PBS-treated and **I)** PGA-Dtx-treated tumor-bearing mice at the experimental endpoint ($n \geq 3$) (yellow star: red pulp; green star: white pulp; blue star: periarteriolar lymphoid nodule; green arrow: multinucleated giant cells). Abbreviations - B: bone; BM: bone matrix; H&E: hematoxylin and eosin.

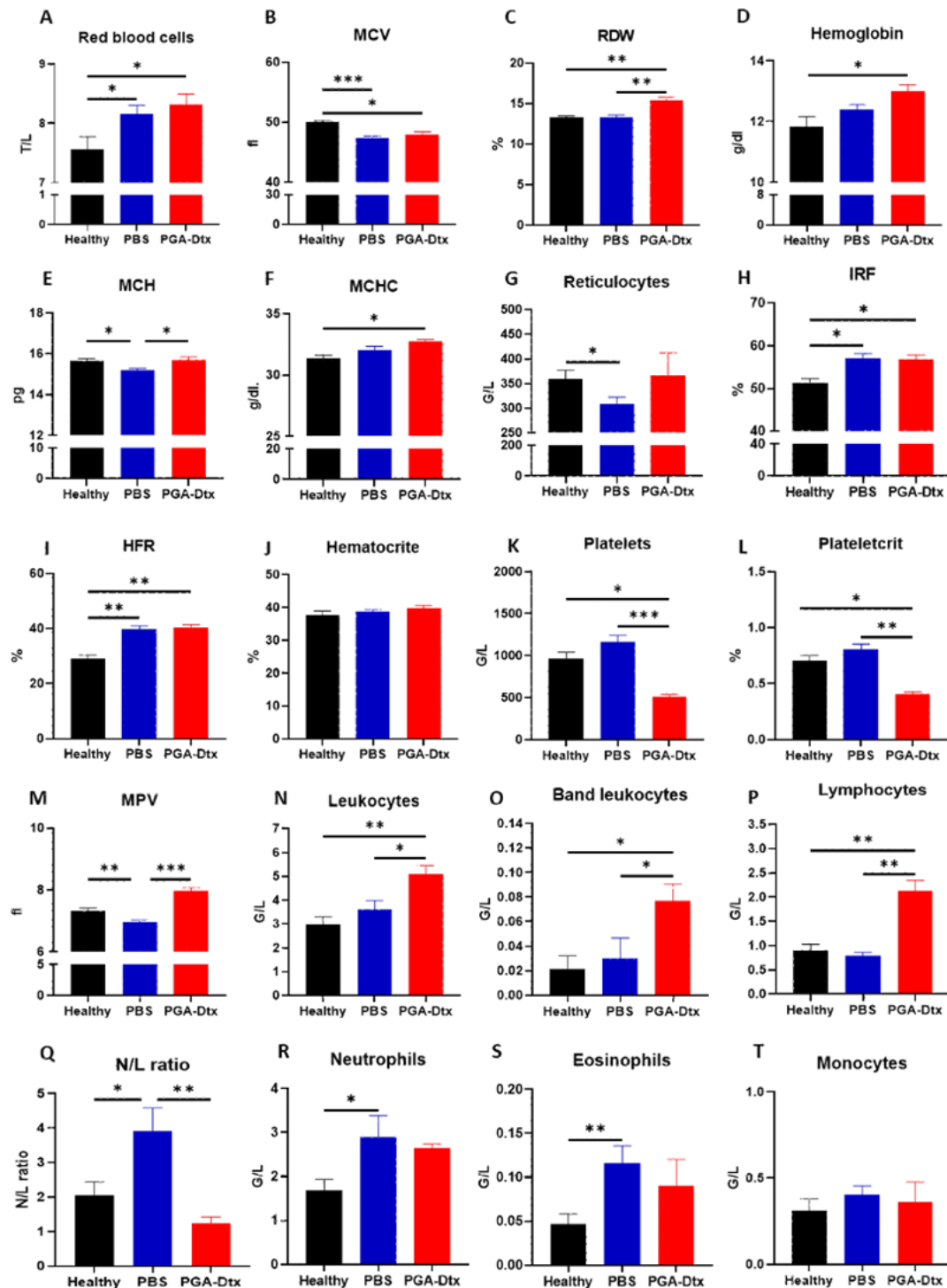


Figure S13. Blood Analysis in the Bone Metastatic Prostate Cancer Mouse Model Following PGA-Dtx Treatment. Levels of **A)** red blood cells, **B)** mean corpuscular volume (MCV), **C)** red cell distribution width (RDW), **D)** hemoglobin, **E)** mean corpuscular hemoglobin, **F)** mean corpuscular hemoglobin concentration (MCHC), **G)** reticulocytes, **H)** immature reticulocyte fraction (IRF), **I)** reticulocyte high-fluorescence ratio (HFR), **J)** hematocrit, **K)** platelets, **L)** plateletcrit, **M)** mean platelet volume (MPV), **N)** leukocytes, **O)** band leukocytes, **P)** lymphocytes, **Q)** neutrophil-to-lymphocyte ratio (N/L ratio), **R)** neutrophils, **S)** eosinophils and **T)** monocytes in healthy and PBS- and PGA-Dtx-treated mice at the experimental endpoint. Abbreviations - %: percentage; fL: femtoliter; g/dL: grams per deciliter; G/L: grams per liter; pg: picograms; T/L: Tera per liter. Data

expressed as mean \pm SEM (n \geq 6). Statistical analysis performed using ANOVA, *p < 0.05, **p < 0.01, ***p < 0.001.

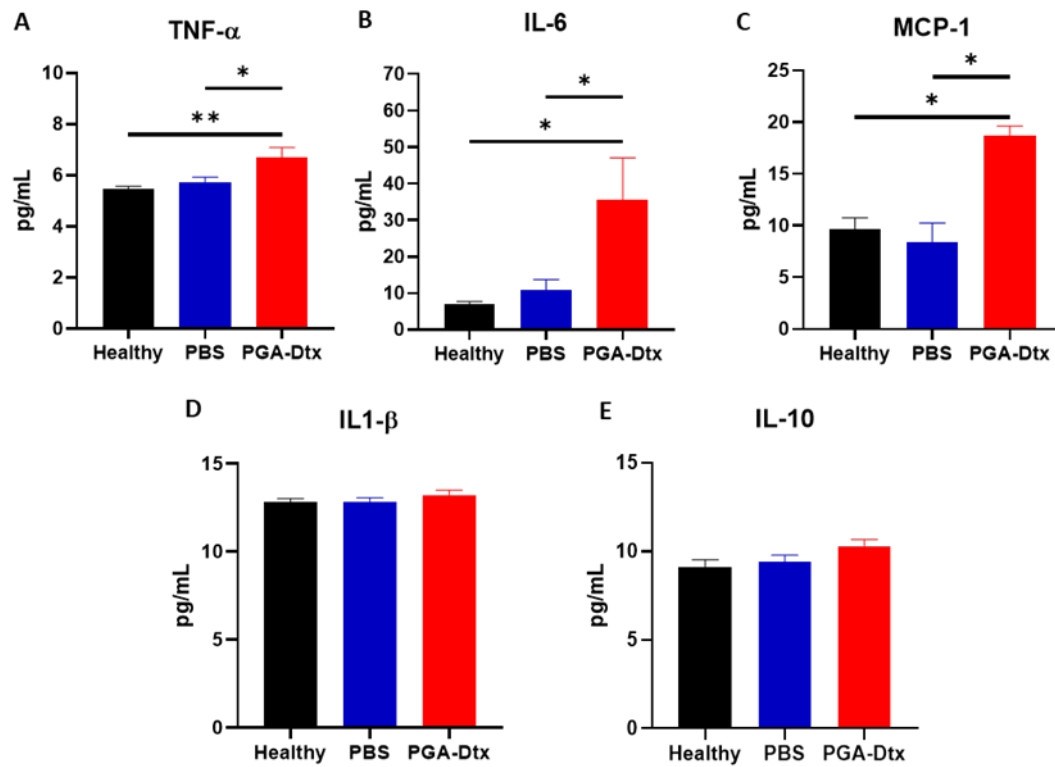


Figure S14. Analysis of Cytokine Levels in the Bone Metastatic Prostate Cancer Mouse Model Following PGA-Dtx Treatment. Serum levels of A) TNF- α , B) IL-6, C) MCP-1, D) IL-1 β , and E) IL-10 in healthy mice and PBS-treated and PGA-Dtx-treated tumor-bearing mice at 4 weeks. Abbreviations - pg/mL: picograms per milliliter. Data expressed as mean \pm SEM (n \geq 5). Statistical analysis performed using ANOVA, *p < 0.05, **p < 0.01.